Journal of Nuclear Materials 403 (2010) 160–166

Contents lists available at ScienceDirect

Journal of Nuclear Materials

journal homepage: www.elsevier.com/locate/jnucmat

Thermo-physical properties of DU–10 wt.% Mo alloys

Douglas E. Burkes [a,*], Cynthia A. Papesch [a], Andrew P. Maddison [a], Thomas Hartmann [b], Francine J. Rice [a]

[a] Idaho National Laboratory, Nuclear Fuels and Materials Division, P.O. Box 1625, Idaho Falls, ID 83415-6188, USA
[b] University of Nevada – Las Vegas, Harry Reid Center for Environmental Studies, 4505 Maryland Parkway Box 454009, Las Vegas, NV 89154-4009, USA

ARTICLE INFO

Article history:
Received 13 March 2010
Accepted 8 June 2010

ABSTRACT

Low-enriched uranium alloyed with 10 wt.% molybdenum is under consideration by the Global Threat Reduction Initiative reactor convert program as a very high density fuel to enable the conversion of high-performance research reactors away from highly-enriched uranium fuels. As with any fuel development program, the thermo-physical properties of the fuel as a function of temperature are extremely important and must be well characterized in order to effectively model and predict fuel behavior under normal and off-normal irradiation conditions. For the alloy system under investigation, the available thermo-physical property data is relatively inconsistent and often lacks appropriate explanation. Available literature on this alloy system comes mainly from studies done during the 1960s and 1970s, and often does not include sufficient information on fabrication history or conditions to draw conclusions for the current application. The current paper has investigated specific heat capacity, coefficient of linear thermal expansion, density, and thermal diffusivity that were then used to calculate alloy thermal conductivity as a function of temperature. The data obtained from this investigation was compared to available literature on similar U–Mo alloys, and in most cases are in good agreement.

1. Introduction

One of the goals of the Global Threat Reduction Initiative (GTRI) reactor convert program has been to develop fuels for nuclear research and test reactors that allow effective core conversion from use of highly-enriched uranium (HEU) fuels to low-enriched uranium (LEU) fuels. By doing so, the threat of a fresh fuel hijacking and subsequent nuclear weapon manufacture will be greatly reduced, effectively minimizing nuclear proliferation worldwide [1]. Uranium alloys that retain the high-temperature γ-phase are ideal for reactor fuel materials, mainly because γ-phase uranium alloys exhibit superior irradiation behavior compared to unalloyed uranium. In addition, γ-phase uranium alloys are ideal for fabrication since many fuel plate fabrication techniques involve elevated temperatures and aluminum, often used as the fuel plate cladding, which has an increased reaction rate in α-phase uranium.

Elements including molybdenum (Mo), niobium (Nb), titanium (Ti), and zirconium (Zr) all exhibit a high degree of solid solubility in *bcc* γ-uranium (U) and are thus often selected as the alloying element(s) [2]. γ-Phase U–Mo alloys are desirable for conversion of research and test reactor fuels mainly because this fuel alloy has excellent resistance to anisotropic growth [3]. Mo also offers a compromise between the necessary amount of alloying element required to stabilize the γ-phase and an acceptable density of U. Density of the fuel is extremely important for reactor core conversion, since a decrease in the fuel enrichment (^{235}U) will require a corresponding increase in the volume of material to maintain the net fissile atom density of the fuel.

The U–Mo alloy system received extensive consideration for fast and thermal reactors in the late 1950s and early 1960s, mainly in the United Kingdom and the US. However, very little work has been conducted on the alloy since then, especially in terms of thermo-physical behavior, both of fresh and irradiated fuel alloys. Great advantages can be gained in thermo-physical property measurement given the advancement in state-of-the-art measurement techniques. This paper discusses the thermo-physical properties of depleted uranium alloyed with ten weight percent molybdenum, referred to as DU–10Mo, which represents the ideal fuel design for the proposed application.

The coefficient of thermal expansion is an important parameter for plate-type nuclear fuels, especially given the current application where the fuel foil is in direct contact with the cladding material. Since the aluminum cladding has a much greater thermal expansion, a precise knowledge of how the fuel will expand is necessary for fuel performance model prediction. Furthermore, coefficient of thermal expansion can be utilized to easily determine the change of alloy density as a function of temperature. Density is a key parameter in determining the fuel conductivity for fuel performance modeling.

Thermal diffusivity is a necessary parameter for determination of thermal conductivity as a function of temperature. Thermal diffusivity of nuclear fuels can also be used to determine safe operating temperatures and aid in process control and quality assurance, ultimately a useful property to lower the cost and increase the

* Corresponding author. Tel.: +1 (202) 586 6062; fax: +1 (202) 586 0239.
E-mail address: Douglas.Burkes@inl.gov (D.E. Burkes).

0022-3115/$ - see front matter © 2010 Published by Elsevier B.V.
doi:10.1016/j.jnucmat.2010.06.018

safety margins associated with nuclear fuel. For the first time to the author's knowledge, measurements to determine the thermal diffusivity of U–Mo alloys as a function of temperature have been made and are discussed in this paper.

Heat capacity is one of the most important thermo-physical properties in determining a fuel's thermal stability [4]. Not only is heat capacity a prerequisite for determination of thermal conductivity, but it is also important in the estimation of stored energy in the fuel during potential accident scenarios.

Thermal conductivity is one of the most important properties of a nuclear fuel. This property ultimately plays a significant role in determining the maximum operating power of a fuel element and the available safety margins. Economics of utilizing the fuel is thereby directly impacted by thermal conductivity. Since this property will change considerably over the lifetime of the element due to the increase in porosity, fission products, and lattice defects, a solid knowledge of the beginning of life (BOL) value is extremely important.

2. Experimental details

2.1. Alloy preparation

A DU–10 wt.% Mo (nominal) alloy was investigated, referred to in this paper as DU–10Mo. Depleted U metal feedstock (<0.21 wt.% ^{235}U, 99.8% purity) and Mo foil (Alfa Aesar, 99.95% purity) were alloyed with a Centorr Model 5SA single arc furnace. The alloyed ingot was melted three times to achieve adequate homogenization, flipping the ingot prior to each melt. The ingot was then melted and cast into a 6.35×10^{-3} m diameter cylindrical graphite book-mold. Inductively Coupled Plasma–Mass Spectrometry (ICP–MS) was utilized to characterize the chemical composition of the casting, indicating a Mo content of 10.3 wt.% with an uncertainty of ±5%. The cylindrical casting was sectioned using a low-speed diamond blade saw. Three samples for laser flash thermal diffusivity (LFTD) were prepared from the casting each approximately 1.5×10^{-3} m long and weighing approximately $0.5–1.0 \times 10^{-3}$ kg. Density of the LFTD samples was determined employing the Archimedes method, revealing an average density of $16.4 \pm 0.1 \times 10^3$ kg m^{-3}. One sample for dilatometry was prepared from the casting approximately 0.023 m long and weighing approximately 0.012 kg. Dimensional measurements on the dilatometry sample produced a density of 16.8×10^3 kg m^{-3}, very close to the measured density for the LFTD samples. The remainder of the casting was used to conduct the as-cast phase analysis. All samples were cleaned in nitric acid and placed in vacuum-sealed bags. The samples were removed from the bags prior to measurement.

Detailed fabrication of the alloy, which was in foil form for the specific heat capacity measurement, can be found in Ref. [5]. The casting process described above was also employed to produce the DU–10Mo ingot by casting into a rectangular graphite book-mold. The coupon was dressed and trimmed to fit into a three-layer 1018 carbon steel picture frame assembly that was welded, and rolled at 923 K to produce a foil approximately 0.254×10^{-3} m thick. The foil was annealed at 923 K for 2 h after rolling was completed. Specimens for heat capacity measurement were prepared by punching circular discs out of the annealed foil, approximately 3×10^{-3} m in diameter. ICP–MS was utilized to characterize the chemical composition of the foil, indicating a Mo content of 10.4 wt.% with an uncertainty of ±5%.

2.2. Phase analysis

X-ray diffraction (XRD) analysis was conducted on a bottom section of the cast slug prepared for dilatometry and LFTD. A second sample for phase analysis was created by sectioning the dilatometer sample after the dilatometry data had been conducted. Measurements both before and after thermo-physical property testing were conducted, using silicon (Si) as an internal standard. Analysis was conducted by scanning from 30 to 100 2θ° simultaneously for a live time of 60 min using an Inel Equinox 1000 diffractometer (Inel, Orleans, France). The X-ray tube operated at a voltage of 30×10^3 V and a current of 30×10^{-3} A. The XRD data were evaluated using Rietveld analysis (Bruker AXS Topas 3). Data obtained from the castings was compared to data for the foil sample, results of which have been previously reported and discussed in Ref. [6].

2.3. Specific heat capacity

Specific heat capacity of the alloy was determined employing a NETZSCH Differential Scanning Calorimeter (DSC) model DSC 404. Platinum (Pt)-rhodium (Rh) crucibles with alumina liners were used to hold the alloy sample and sapphire reference material for analysis. Ultra-high purity argon (Ar) cover gas passed through an oxygen gettering furnace (OxyGon Industries, Inc. Model OG-120 M). Oxygen impurity levels were in the sub *ppb* range based on the measurability of the furnace. A flow rate of 0.33×10^{-3} L s^{-1} was established for the sample furnace. Three consecutive DSC runs were conducted from ambient temperature to approximately 1073 K, each followed by controlled cooling to ambient temperature. A heating rate of 0.167 K s^{-1} was utilized for both the heating and cooling cycles. Data was collected during both heating and cooling. Specific heat capacity was determined by employing a sapphire standard curve produced prior to every sample run and NETZSCH Proteus Thermal Analysis software that is based on ASTM Standard E 1269-05 [7].

2.4. Dilatometry

A Netzsch model DIL 402-E dilatometer was utilized for coefficient of linear thermal expansion techniques. Data was collected from room temperature to 1073 K for both heating and cooling in following ASTM E 228-06 [8] as a reference. Three subsequent heating and cooling cycles were performed on a sample representing each alloy. Both the heating and cooling rates during the measurement were 0.042 K s^{-1}. Helium (He) cover gas flowing through the chamber at 0.83×10^{-3} L s^{-1} was used to minimize sample oxidation at elevated temperatures. Values of the instantaneous coefficient of linear thermal expansion and the engineering coefficient of linear thermal expansion were determined from the dilatometer curves as a function of temperature. Density change of each alloy as a function of temperature was calculated by assuming isotropic expansion, the calculated percent of linear thermal expansion, and the average density at room temperature determined using the Archimedes method on the LFTD samples.

2.5. Laser flash thermal diffusivity

Thermal diffusivity measurements were performed utilizing an Anter Corporation Laser Flash Diffusivity instrument model FL5000. Ultra-high purity Ar cover gas that passed through an Oxy Gon Industries, Inc. Model OG-120 M oxygen gettering furnace was used during the measurements. Oxygen impurity levels were in the sub *ppb* range based on the internal calibration of the gettering furnace. Measurements were made from 473 to 1073 K in 100 K increments (along with a measurement at 323 K) upon heating for each alloy composition following ASTM E 1461-07 [9] as a reference. Four to six shots were taken at each temperature. The Clark and Taylor approximation method was employed to deter-

mine the thermal diffusivity of the sample at temperature based on the half-rise time.

3. Results and discussion

3.1. Phase analysis

XRD patterns of the DU–10Mo as-cast (pre-measurement) alloy, the as-rolled (pre-measurement) foil, and heat-treated (post-measurement) as-cast alloy are shown in Fig. 1. The patterns are normalized to the maximum intensity peak in each pattern to show a clear distinction in reflection intensity. Results of the quantitative analysis along with the lattice parameter determination of γ-U(Mo) is provided in Table 1. The lattice parameter determinations all show a rather small standard deviation below 0.1×10^{-3} nm. Rietveld analysis of the XRD measurements resulted in refinement residuals between 7.4% and 16.2% for the cast alloys that are larger than typically desired and are attributed to the nature of the bulk samples that were measured. The as-cast and heat-treated samples have a significant amount of peak broadening compared to the as-rolled sample. The rougher surface of the as-cast and heat-treated samples, prepared by low-speed sectioning, contributes to the peak broadening and allows additional undesired effects, such as surface texture, preferred orientation, etc. Furthermore, different equipment and acquisition times were utilized for the as-rolled sample than for the as-cast and heat-treated samples, which to a small degree will also contribute to differences in the peak sharpness.

The lattice parameter for the as-cast sample decreased slightly post-measurement and was comparable to the lattice parameter of the as-rolled sample. An increase in the Mo solid substitution on the *bcc* γ-U lattice will result in a lattice parameter decrease.

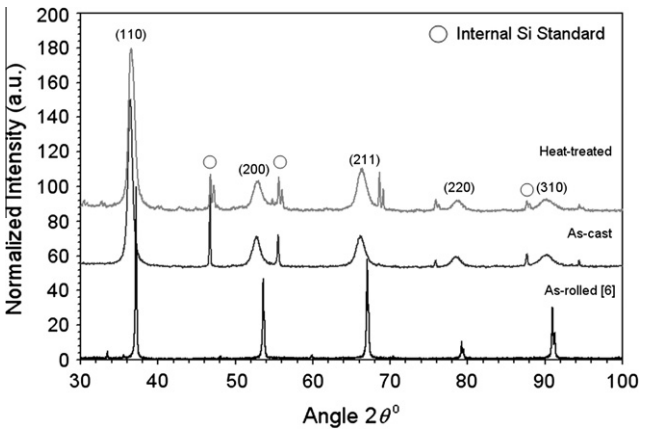

Fig. 1. X-ray diffraction patterns of the DU–10Mo alloy before (as-cast) and after (heat-treated) dilatometer measurement and an X-ray diffraction pattern for an as-rolled sample. The expected γ-U(Mo) phase is the major phase in all patterns. However, minor amounts of α-U(Mo), γ^0-U_2Mo, and surface UO_2 phases are also present.

The decrease in the lattice parameter for the as-cast alloy suggests improved homogenization of the alloy upon heat treatment during the dilatometer thermal cycles. The larger lattice parameter for the as-cast (pre-measurement) sample suggests that the quenching of the γ-U(Mo) hard solution resulted in a metastable γ^s-phase [12]. Improved homogenization of the alloy during the dilatometer run will result in a decreased distance between the long and the short bonds of the γ^s pseudocell that will more closely match an ideal *bcc* lattice for γ-U(Mo). Furthermore, there is a slight reduction in both the α-U(Mo) and intermetallic U_2Mo phases from the as-cast sample as a result of cycling through the dilatometer. The fact that the amount of α-U(Mo) and U_2Mo phase does not increase confirms that the relatively longer thermal cycles associated with the dilatometry measurement and lower heating/cooling rates does not result in decomposition of the γ-U(Mo) phase, owing to the extremely sluggish diffusion characteristics of this particular alloy system. Numerous Time–Temperature-Transformation (TTT) diagrams available in literature suggest on the order of tens of hours at 823 K before onset of γ-phase decomposition occurs [13–15]. None of the samples were exposed at temperatures approaching the eutectoid temperature for more than a few hours cumulatively, such that significant decomposition was not expected, or observed, to occur.

In general, the lattice parameter determinations for these samples are close to values available in literature. In each case, values from the current work are slightly higher than those in the literature. The slightly larger lattice parameters of the current work are attributed to differences in the measurement technique and the fact that alloys in the current work are slightly off the nominal target composition by 0.3–0.4 wt.% Mo.

3.2. Sample runs

Fig. 2 gives an example of a typical DSC and dilatometer trace for the DU–10Mo alloy. For the most part, the DSC traces were reproducible and consistent with each measurement cycle. The first DSC trace was slightly different upon heating compared to the subsequent heating runs suggested to occur from improved homogenization and further annealing of residual stress imparted by the rolling process. The DSC cooling traces are consistent with one another after the first heating run to 1073 K. It is important to point out that there are no phase changes evident from the DSC traces suggesting that the γ-phase is stable upon heating.

Similarly, the dilatometer traces show that the first run is slightly different from the two subsequent runs suggested to occur from improved homogenization of the alloy and alleviation of residual stresses present from the casting process. Runs 2 and 3 showed a slight increase (~0.25%) in expansion upon heating onset at 523 K that is not reproduced upon cooling. The reason for this slight increase is not well understood at this time, but could be the result of improved homogenization of the sample with each thermal cycle. The slight increase is not associated with decomposition of the γ-U(Mo) phase based on the XRD studies performed prior to and after the measurement. The dilatometer traces show expected linear behavior upon both heating and cooling. A small

Table 1
Phase content analysis and lattice parameter determination of the as-cast and as-rolled alloys before measurement and the as-cast alloy after (heat-treated) dilatometer measurement.

DU–10Mo alloy	γ-U(Mo) content (wt.%)	α-U(Mo) content (wt.%)	γ^o-U_2Mo content (wt.%)	UO_2 content (wt.%)	γ-U(Mo) lattice parameter (nm)	
					This work	Literature
As-CAST, pre-measurement	90.4 ± 1.2	2.8 ± 0.5	6.8 ± 1.4	–	0.34269 ± 0.00003	
As-rolled pre-measurement	98.1 ± 0.2	–	–	1.9 ± 0.2	0.34155 ± 0.00008	0.34129 [10] 0.3415 [11]
As-CAST, post-measurement	93.5 ± 1.6	1.1 ± 0.4	4.9 ± 1.1	–	0.34188 ± 0.00006	

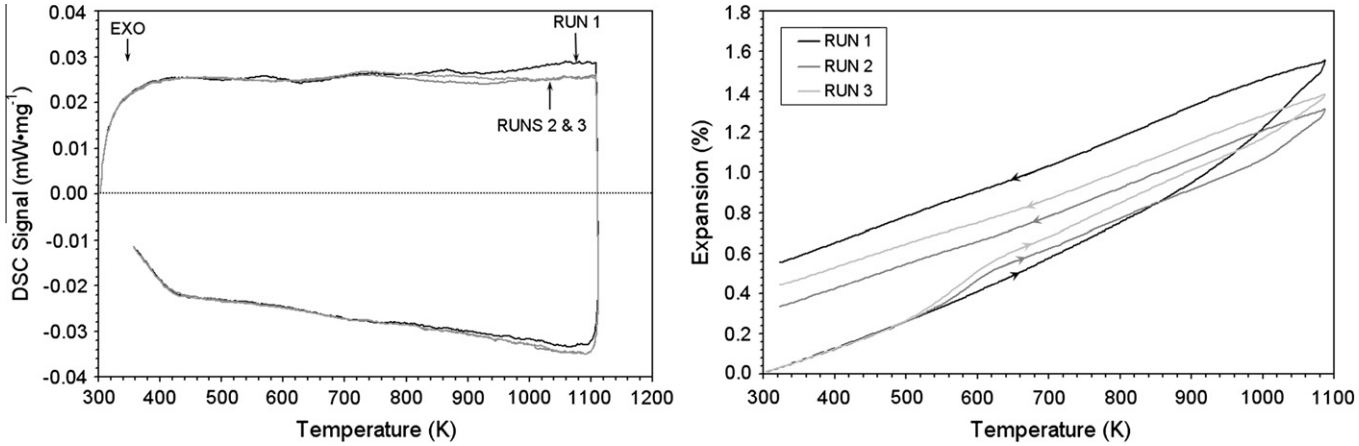

Fig. 2. DSC (left) and dilatometer (right) traces for the DU–10Mo alloy obtained for both heating and cooling.

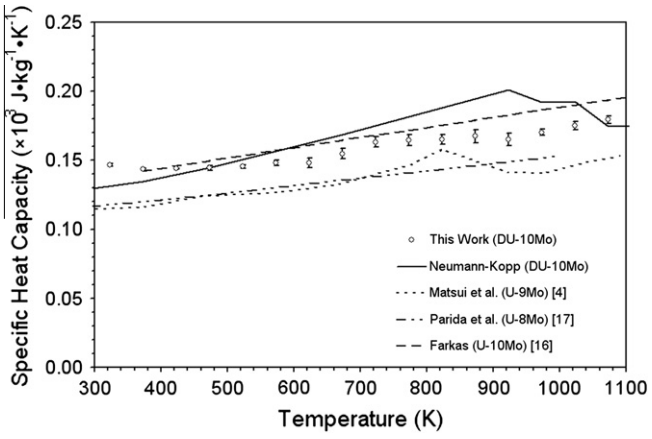

Fig. 3. Measured specific heat capacities for the DU–10Mo alloy as a function of temperature and compared to values obtained from literature on similar alloys.

hysteresis exists upon cooling that can most likely be attributed to the Mo redistribution, the alleviation of residual stresses present from the casting process, and the disorder associated with the γ-U(Mo) solid solution.

3.3. Specific heat capacity

The measured specific heat capacity for the DU–10Mo alloy is shown in Fig. 3. The specific heat capacity is relatively constant from room temperature to 623 K (0.146×10^3 J kg^{-1} K^{-1}) and then begins to increase near linearly with further increased temperature. Included on the figure are heat capacity values determined from similar alloys published in available literature. Observation of the figure reveals that there is relatively good agreement between the data collected as part of this work and data available from literature, particularly with the only other data available on a U–10Mo alloy [16]. The values obtained by Parida et al. on a U–8Mo alloy [17] and by Matsui et al. on a U–9Mo alloy [4] are close to one another and lower than that of the current work. In general, the heat capacity should decrease with increased Mo, due to the lower heat capacity value of Mo compared to U. The specific heat capacity running counter to the expected trend for Parida et al. [17] and Matsui et al. [4] most likely results from differences in the sample preparation and measurement techniques. Matsui et al. homogenized their alloy at 773 K for 3 days followed by slow cooling [4], while Parida et al. homogenized their alloy at 1223 K for 120 h followed by water quenching [17], where samples in the current work were not homogenized prior to measurement. The slow cooling of Matsui et al. alloy resulted in a two-phase mixture of α-U and γ′-U_2Mo and the authors attributed the difference between the heat capacity of Mo and that of γ′-U_2Mo as the driver for the lower heat capacity [4]. Parida et al. employed a Calvert calorimeter to perform enthalpy measurements from which heat capacity was obtained [17]. The difference in the measurement method and technique could very easily cause the specific heat capacity to be lower than expected, although the authors do not discuss why their measurements are lower than those predicted by the Neumann–Kopp approximation.

An approximated value for the U–10Mo alloy employing the Neumann–Kopp rule is also provided in Fig. 3. Values for the Neumann–Kopp approximation will not be entirely accurate since α-U is used in the calculation from room temperature to 942 K, β-U from 942 to 1049 K, and finally γ-U above 1049 K. The values in available literature and the DU–10Mo alloy from the current work all follow a similar trend as that predicted by the Neumann–Kopp approximation, short of the transitions associated with $\alpha \rightarrow \beta \rightarrow \gamma$. The specific heat capacity of the DU–10Mo alloy closely matches the Neumann–Kopp approximation above 1073 K – once the alloy is composed only of γ-phase. The specific heat capacity of U–10Mo can be represented by Eq. (1), obtained through regression analysis using data from Farkas [16] and the current work, where $c_{p,U-10Mo}$ is in J kg^{-1} K^{-1} and T is in K.

$$c_{p,U-10Mo} = (0.113 \times 10^3 \pm 4.28) + (7.05 \times 10^{-2} \pm 5.20 \times 10^{-3}) \cdot T \quad (1)$$

3.4. Thermal expansion and density

The instantaneous coefficient of linear thermal expansion was determined from the dilatometer runs and average values are provided in Fig. 4. Also included in the figure are instantaneous coefficients of linear thermal expansion available from published literature for comparable alloys. In general, average instantaneous coefficients of linear thermal expansion for the DU–10Mo alloy obtained in the current work are slightly higher than those obtained for similar alloys in published literature. Values obtained for the DU–10Mo alloy upon heating are very similar to those presented by Saller et al. up to the temperature range 300–1073 K [18]. Values upon cooling are very similar to the only other available data on a U–10 wt.% Mo alloy [19]. The literature values are presented as a comparison to the current work and to serve as a baseline and historical reference for any future measurements.

The engineering coefficients of linear thermal expansion calculated from the dilatometer runs are provided in Fig. 5. The engi-

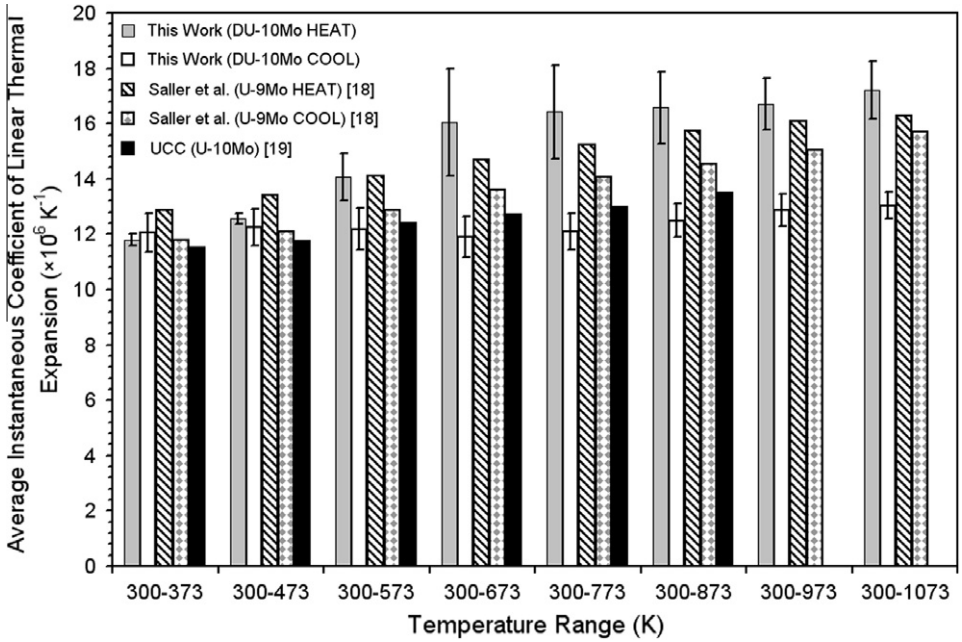

Fig. 4. Average instantaneous coefficients of linear thermal expansion for the DU–10Mo alloy as a function of temperature and compared to values obtained from literature for similar alloys.

neering coefficient of linear thermal expansion for the DU–10Mo alloy investigated in this work compares reasonably well with those obtained for a U–10 wt.% Mo alloy by Klein [20] up to 823 K. Above 823 K, the values from Klein are higher than the alloy in the current work. This could result from variations between actual and nominal alloy composition, test method, Mo redistribution, and/or phases present during analysis, but this information is not accessible from the previous literature. However, based on the nature of the deviation and the inflection point from 823 to 873 K for the data of Klein [20], the difference for the DU–10Mo alloy of the current work and that of Klein is most likely the result of γ-U(Mo) phase decomposition.

The theoretical density of a DU–10Mo alloy based on the rule of mixtures is $17.06 \times 10^3\ \mathrm{kg\,m^{-3}}$. Dimensional measurements on the dilatometry sample resulted in a density of $16.75 \times 10^3\ \mathrm{kg\,m^{-3}}$, suggesting there is less than 2% porosity in the sample. Immersion density measurements on the LFTD samples resulted in an average density of $16.4 \pm 0.1 \times 10^3\ \mathrm{kg\,m^{-3}}$, suggesting a porosity of approximately 3.8%. The small amount of porosity that may be present is not expected to have a significant influence on the density change of the alloy as a function of temperature, but could have contributed to the small hysteresis between heating and cooling observed during the dilatometer runs. McGeary [21] determined a room temperature density of $17.2 \times 10^3\ \mathrm{kg\,m^{-3}}$ for a U–10 wt.% Mo alloy, higher than the theoretical value based on the rule of mixtures. No explanation for this observation is available from the literature.

Density as a function of temperature for each alloy was calculated based on the average percent of expansion and the average density of the alloy at room temperature determined from the Archimedes method on the LFTD samples, as shown in Fig. 6. Error in the density calculations is carried by the deviation in the amount of expansion measured upon cycling the alloy three times between room temperature and 1073 K and from the deviation in the immersion density measurements. Average density determined from the LFTD samples was used since this value encom-

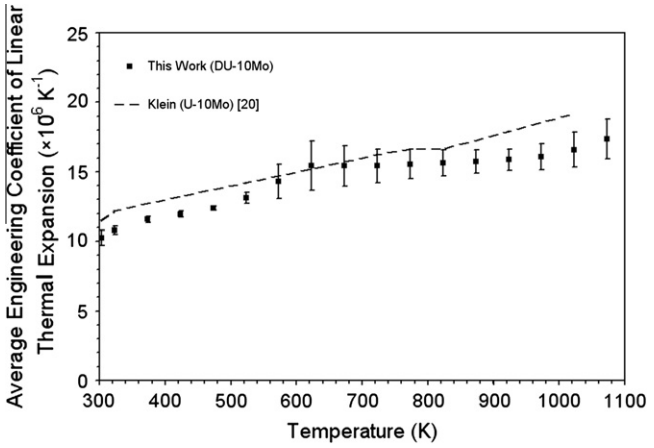

Fig. 5. Average engineering coefficients of linear thermal expansion for the DU–10Mo alloy as a function of temperature and compared to values obtained from literature for a similar alloy.

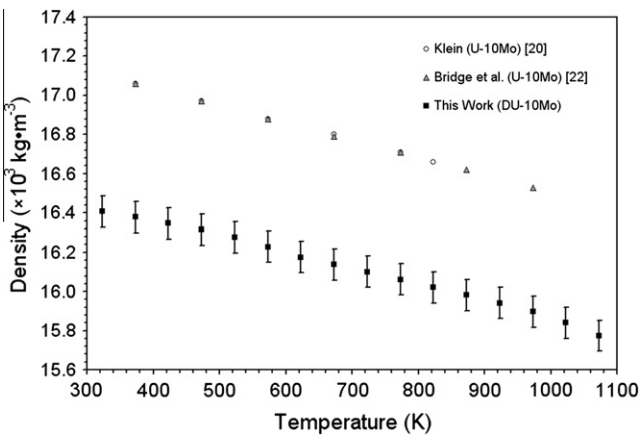

Fig. 6. Calculated density of the DU–10Mo alloy as a function of temperature and compared to values obtained from literature on similar alloys.

passes the LFTD measurements and the dimensional measurements conducted on the dilatometry sample. Corrections for porosity will be applied to thermal conductivity later in the paper. Density decreased near linearly with increasing temperature. The values calculated for the DU–10Mo alloy in the current work follow a near identical trend but are approximately 4% lower than those determined for a similar U–10 wt.% Mo alloy by Klein [20] and Bridge et al. [22]. This deviation is attributed directly to the porosity of the alloy used in the calculations (~3.8%) and the fact that the previous measurements must have been conducted on fully dense samples. The lack of experimental details does not allow confirmation of how or if porosity was determined and factored for those measurements. The density of U–10Mo can be represented by Eq. (2) based on the data presented in Fig. 6, where ρ_{U-10Mo} is in kg m^{-3}, $\rho_{RT,U-10Mo}$ is the room temperature density of the alloy, and T is in K.

$$\rho_{U-10Mo} = \rho_{RT,U-10Mo} - (8.63 \times 10^{-4} \pm 2.76 \times 10^{-5}) \cdot T \quad (2)$$

3.5. Thermal diffusivity

Calculated average thermal diffusivity employing the Clark and Taylor approximation as a function of temperature for the alloy is provided in Fig. 7. The measurements were not corrected for porosity at this time. In general, the dependence of thermal diffusivity on temperature increases modestly from room temperature to approximately 873 K and then levels off. To the author's knowledge, this is the first time that thermal diffusivity of U–Mo alloys has been measured and presented in the open literature. Thus, there are no values available to compare against the current results. The data is best represented by a second-order polynomial that follows Eq. (3), where α is in m^2 s^{-1} and T is temperature from 323 to 1073 K.

$$\alpha = (-2.30 \times 10^{-6} \pm 1.00 \times 10^{-6}) + (2.75 \times 10^{-8} \pm 3.05 \times 10^{-9}) \cdot T - (1.25 \times 10^{-11} \pm 2.14 \times 10^{-12}) \cdot T^2 \quad (3)$$

3.6. Thermal conductivity

Thermal conductivity (λ) as a function of temperature for the alloy was calculated using the specific heat capacity (c_p), thermal diffusivity (α), and density (ρ) data obtained from this work and Eq. (4).

$$\lambda = \alpha \cdot \rho \cdot c_p \quad (4)$$

Linear propagation of error calculations were computed based on the standard deviations in the measurement of each property. For small volume fractions of inclusions, i.e., <15 vol.%, the Maxwell–Eucken expression can be used to describe the thermal conductivity of an arrangement of isolated spherical inclusions dispersed in a continuous homogeneous matrix, represented in Eq. (5) [23,24].

$$\lambda_{eff} = \lambda_m \left[\frac{\lambda_i + 2\lambda_m + 2v_i(\lambda_i - \lambda_m)}{\lambda_i + 2\lambda_m - v_i(\lambda_i - \lambda_m)} \right] \quad (5)$$

In Eq. (5), λ_{eff} is the effective thermal conductivity of the sample, λ_m is the thermal conductivity of the continuous homogeneous matrix, λ_i is the thermal conductivity of the spherical inclusion phase, and v_i is the volume fraction of the spherical inclusion phase dispersed throughout the continuous homogeneous matrix. Eq. (5) assumes that the spherical inclusions are located sufficiently far from one another such that they do not interact to permit the establishment of a thermal connected path, i.e., percolation [25]. Furthermore, the inclusions, or pores in this case, are assumed to be filled with air therefore having a thermal conductivity of zero (negligible when compared to the matrix thermal conductivity), are of micron size, and are well dispersed throughout the matrix. The experimental thermal conductivity was corrected for the approximated porosity of the DU–10Mo alloy, as determined by Archimedes method on the LFTD sample taken as the volumetric fraction of porosity, by substituting values for λ_{eff} and v_i into Eq. (5), and solving for λ_m. The corrected thermal conductivity values for the alloy are presented in Fig. 8. Also included on Fig. 8 are thermal conductivity values available from published literature.

In general, values for the current work fall within a similar range as the data presented in the literature for U–Mo alloys with Mo contents varying from 9 to 11 wt.% Mo. Furthermore, the thermal conductivity determined from the current work shows similar temperature dependence up to 873 K when compared to literature values. However, when compared to thermal conductivity of other U–10Mo alloys, the values from the current work tend to be roughly 20% higher. The thermal conductivity of U–10Mo can be represented by Eq. (6), obtained through regression analysis using data from Klein [20], McGeary [21], Touloukian et al. [27], and the current work, where λ_{U-10Mo} is in W m^{-1} K^{-1} and T is in K.

$$\lambda_{U-10Mo} = (0.606 \pm 1.08) + (3.51 \times 10^{-2} \pm 1.61 \times 10^{-3}) \cdot T \quad (6)$$

It is apparent from the literature values provided in Fig. 8 that there is no clear dependence of thermal conductivity on Mo content. Values measured by Konobeevskii [26] on a U–9Mo alloy appear to have an unusually strong dependence upon temperature for these types of alloys. In most cases, the thermal conductivity of the alloys from previous literature were determined from elec-

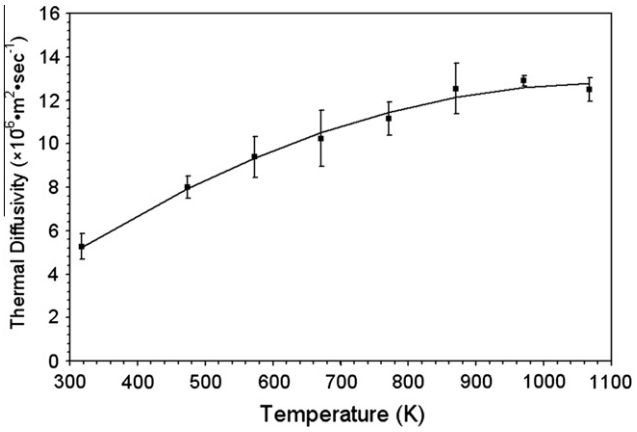

Fig. 7. Average thermal diffusivity as a function of temperature.

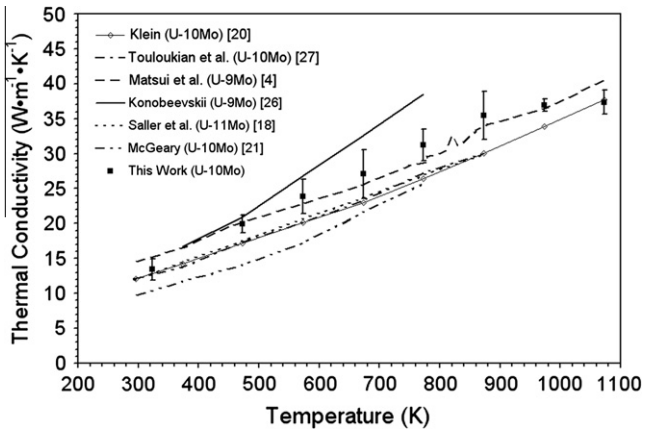

Fig. 8. Thermal conductivity computations based on specific heat capacity, thermal diffusivity, and density measurements for the DU–10Mo alloy as a function of temperature and compared to values obtained from literature on similar alloys.

trical conductivity measurements and converted using the Wiedemann–Franz law. Thermal conductivity measurements obtained from electrical conductivity should be lower than those measured in a direct or semi-direct manner, since electrical conductivity only considers the electronic contribution to thermal conductivity and phonon–phonon scattering is not taken into account. It must also continue to be noted that in the case of older literature, the experimental method and resultant phase analysis of the alloys investigated is not always available or clear. This makes determination of any potential Mo and/or phase effect on the resultant data very challenging.

4. Conclusions

LEU alloys consisting of 10 wt.% Mo is being considered by the GTRI reactor convert program as a very high density fuel to enable the conversion of high-performance research reactors away from the use of HEU fuels. Thermo-physical properties are an important part of any fuel development campaign. As such, the specific heat capacity, coefficients of linear thermal expansion, density, thermal diffusivity, and thermal conductivity have been determined on a representative fuel alloy system as a function of temperature. The data obtained on the representative alloy was compared with previously published values in literature. The values obtained from this work are in good agreement with previously published values, with most variations being explained by changes in measuring technique, experimental method, or sample fabrication procedure. Understanding the thermo-physical properties of this potential fuel alloy will greatly aid development of higher fidelity models and assist with the interpretation of performance for this particular application since the thermo-physical properties will degrade significantly with irradiation and burnup.

US department of energy disclaimer

Acknowledgements

This work was supported by the US Department of Energy (DOE) and the National Nuclear Security Administration (NNSA) under DOE Idaho Operations Office Contract DE-AC07-05ID14517. Accordingly, the US Government retains a nonexclusive, royalty-free license to publish or reproduce the published form of this contribution, or allow others to do so, for US Government purposes.

The authors are appreciative of the Fuels and Applied Sciences Building and Analytical Laboratory staff at the Materials and Fuels Complex of Idaho National Laboratory. The authors specifically wish to acknowledge Mr. Glenn Moore and Mr. Steve Steffler for fabrication of the alloy specimens, and Mr. Bryan Forsmann and Mr. Spencer Taylor for their assistance with material transfers and immersion density measurements.

References

[1] J.L. Snelgrove, G.L. Hofman, M.K. Meyer, C.L. Trybus, T.C. Wiencek, Nucl. Eng. Des. 178 (1997) 119–126.
[2] G.L. Hofman, L.C. Walters, in: B.R.T. Frost (ed.), Materials Science Technology, Nuclear Materials, vol. 10A, VCH, New York, 1994.
[3] J.H. Kittel, B.R.T. Frost, J.P. Mustelier, K.Q. Bagley, G.C. Crittenden, J. Van Dievoet, J. Nucl. Mater. 204 (1993) 1–13.
[4] T. Matsui, T. Natsume, K. Naito, J. Nucl. Mater. 167 (1989) 152–159.
[5] C.R. Clark, G.C. Knighton, M.K. Meyer, G.L. Hofman, Monolithic Fuel Plate Development at Argonne National Laboratory, 2003 International Meeting on Reduced Enrichment for Research and Test Reactors, Chicago, IL, 2003, pp. 1-10.
[6] D.E. Burkes, T. Hartmann, R. Prabhakaran, J.-F. Jue, J. Alloys Compd. 479 (2009) 140–147.
[7] ASTM E 1269-05, Standard Test Method for Determining Specific Heat Capacity by Differential Scanning Calorimetry, 2005.
[8] ASTM E 228-06, Standard Test Method for Linear Thermal Expansion of Solid Materials with a Push-Rod Dilatometer, 2006.
[9] ASTM E 1461-07, Standard Test Method for Thermal Diffusivity by the Flash Method, 2007.
[10] A.E. Dwight, J. Nucl. Mater. 2 (1) (1960) 81–87.
[11] A.M. Nomine, D. Bedere, D. Miannay, The influence of physio-chemical parameters on the mechanical properties of some isotropic uranium alloys, in: Proceedings of the Third Army Materials Technical Conference, Physical Metallurgy of Uranium Alloys, Vail, CO, 1974, pp. 657–699.
[12] V.K. Orlov, V.M. Teplinskaya, N.T. Chebotarev, Atom. Energy 88 (2000) 42–47.
[13] R.J. Van Thyne, D.J. McPherson, Trans. ASM 49 (1957) 598.
[14] C.A.W. Peterson, W.J. Steele, S.L. Digiallonardo, Isothermal transformation study of some uranium-base alloys, Report UCRL-7824, 1964.
[15] P.E. Repas, R.H. Goodenow, R.F. Hehemann, Trans. ASM 57 (1964) 150.
[16] M.S. Farkas, Mechanical and physical properties of fuels and cladding materials with potential for use in Brookhaven's pulsed fast reactor, Report BMI-X-455, 1967.
[17] S.C. Parida, S. Dash, Z. Singh, R. Prasad, V. Venugopal, J. Phys. Chem. Solids 62 (2001) 585–597.
[18] H.A. Saller, R.F. Dickerson, W.E. Muir, Uranium Alloys for High Temperature Application, BMI-1098, June 25, 1956, pp. 24–27.
[19] Union Carbide Corporation, Metallurgy Division Annual Progress Report for the Period Ending May 31, 1961, ORNL-3160, 1961.
[20] J.L. Klein, in: A.R. Kaufmann (Ed.), Nuclear Reactor Fuel Elements, Wiley, New York–London, 1962, p. 31 (Chapter 3).
[21] R.K. McGeary (Ed.), Development and Properties of Uranium-Base Alloys Corrosion Resistant in High-Temperature Water, Pt. I., Alloys Without Protective Cladding, WAPD-127, 1955.
[22] J.R. Bridge, C.M. Schwartz, D.A. Vaughan, Trans. AIME 206 (1956) 1282; L.T. Lloyd, Trans. AIME 209 (1957) 532.
[23] N.S. Sundarmurti, V. Rao, ISIJ Int. 42 (7) (2002) 800–802.
[24] J.C. Maxwell, Treatise on Electricity and Magnetism, first ed., Clarendon Press, Oxford, 1873.
[25] A. Eucken, Forsch. Geb. Ing., B-3, Forschung Sheft 53 (1932) 6–21.
[26] S.T. Konobeevskii, Some physical properties of uranium, plutonium, and their alloys, in: Proceedings of the Second UN International Conference on the Peaceful Uses of Atomic Energy, Paper P/2230, 1958.
[27] Y.S. Touloukian, R.W. Powell, C.Y. Ho, P.G. Klemens, Thermophysical Properties of Matter, vol. 1, IFI/Plenum, New York, 1970.